

Rochester Institute of Technology

## RIT Digital Institutional Repository

---

Articles

Faculty & Staff Scholarship

---

12-1-2004

### The V1647 Orionis (IRAS 05436–0007) Protostar and Its Environment

Peregrine M. McGehee  
*Los Alamos National Laboratory*

J. Allyn Smith  
*Los Alamos National Laboratory*

Arne A. Henden  
*Universities Space Research Association and US Naval Observatory*

Michael Richmond  
*Rochester Institute of Technology*

Gillian R. Knapp  
*Princeton University Observatory*

*See next page for additional authors*

Follow this and additional works at: <https://repository.rit.edu/article>

---

#### Recommended Citation

Peregrine M. McGehee et al 2004 ApJ 616 1058 <https://doi.org/10.1086/425069>

This Article is brought to you for free and open access by the RIT Libraries. For more information, please contact [repository@rit.edu](mailto:repository@rit.edu).

---

## Authors

Peregrine M. McGehee, J. Allyn Smith, Arne A. Henden, Michael Richmond, Gillian R. Knapp, Douglas P. Finkbeiner, and J. Brinkmann

# The V1647 Ori (IRAS 05436-0007) Protostar And Its Environment

Peregrine M. McGehee<sup>1,2</sup>, J. Allyn Smith<sup>3,4</sup>, Arne A. Henden<sup>5</sup>, Michael W. Richmond<sup>6</sup>,  
Gillian R. Knapp<sup>7</sup>, Douglas P. Finkbeiner<sup>7</sup>, Željko Ivezić<sup>7</sup>, J. Brinkmann<sup>8</sup>

peregrin@apo.nmsu.edu

## ABSTRACT

We present Sloan Digital Sky Survey and United States Naval Observatory observations of the V1647 Ori protostar and surrounding field near NGC 2068. V1647 Ori, the likely driving source for HH 23, brightened significantly in November 2003. Analysis of SDSS imaging acquired in November 1998 and February 2002 during the quiescent state, recent USNO photometry, and published 2MASS and Gemini data shows that the color changes associated with brightening suggest an EXor outburst rather than a simple dust clearing event.

*Subject headings:* stars: formation - stars: pre-main-sequence - stars: circumstellar matter - stars: individual (V1647 Ori, IRAS 05436-0007)

---

<sup>1</sup>Los Alamos National Laboratory, LANSCE-8, MS H820, Los Alamos, NM 87545

<sup>2</sup>Department of Astronomy, New Mexico State University, MSC 4500, Box 30001, Las Cruces, NM 88003

<sup>3</sup>Los Alamos National Laboratory, ISR-4, MS D448, Los Alamos, NM 87545

<sup>4</sup>Department of Physics & Astronomy, University of Wyoming, 1000 E. University Blvd., Laramie, WY 82071

<sup>5</sup>Universities Space Research Association/US Naval Observatory, Flagstaff Station, P.O. Box 1149, Flagstaff, AZ 86002

<sup>6</sup>Department of Physics, Rochester Institute of Technology, 85 Lomb Memorial Drive, Rochester, NY 14623

<sup>7</sup>Princeton University Observatory, Princeton, NJ 08544

<sup>8</sup>Apache Point Observatory, 2001 Apache Point Road, Sunspot, NM 88349

## 1. Introduction

In January 2004, J.W. McNeil discovered a new reflection nebula in the dark cloud Lynds 1630 near M 78 (McNeil 2004). This object, now known as McNeil’s Nebula, is apparently associated with an EXor-type eruption (Reipurth & Aspin 2004) of the embedded protostar V1647 Ori.

EXors belong to the class of pre-main-sequence optical variables (Herbig 1977). They are classical T Tau stars which undergo irregular outbursts in the optical/UV of several magnitudes, named for the prototype EX Lup (Herbig et al. 2001). These outbursts are interpreted as episodes of substantial mass transfer resulting from instabilities in the accretion disk; they are present very early in the evolution of a protostar, as shown by the detection of EXor outbursts from deeply embedded Class 1 protostars in the Serpens star formation region (Hodapp et al. 1996).

Clark (1991) first identified V1647 Ori as the young stellar object IRAS 05436-0007 on the basis of its IRAS colors. I-band and [SII] narrow-band imaging of the region by Eisloffel & Mundt (1997) revealed a faint I band source at the position of the IRAS object and reflection nebulosity extending to the north, identifying V1647 Ori as the likely driver for HH 23, located 170 arcsec north of the star. The bolometric flux of the source derived from IRAS and sub-millimeter photometry by Lis, Menten, & Zylka (1999) yields a luminosity of  $2.7 L_{\odot}$  and an inferred molecular gas mass of  $0.4 M_{\odot}$  assuming a distance of 400 pc to the Orion star-forming complex (Anthony-Twarog 1982).

Estimates of the extinction towards V1647 Ori,  $A_V = 11^m - 15^m$ , are found to be similar from photometry taken during the quiescent phase (Abraham et al. 2004) and during the eruptive phase (Reipurth & Aspin 2004; Vacca et al. 2004; Briceño et al. 2004; Andrews, Rothberg & Simon 2004). Thus, it is not clear whether the appearance of McNeil’s Nebula is due only to the eruption of V1647 Ori or to the eruption plus additional clearing of obscuring circumstellar dust. In this paper, we examine this question using pre-eruption multiband optical and near infrared data from the Sloan Digital Sky Survey (SDSS) and the Two Micron All Sky Survey (2MASS) compared with post-eruption data in the SDSS and 2MASS bands observed at the United States Naval Observatory.

## 2. Observations

We detect the protostar at four epochs of Sloan Digital Sky Survey (SDSS) imaging as a point source (SDSS J054613.14-000604.1) coincident with the 2MASS *K*-band position ( $\alpha_{2000}=05^h46^m13.1^s$ ,  $\delta_{2000}=-00^{\circ}06'05''$ ). The SDSS observations consist of two pairs of scans

acquired in November 1998 and February 2002. Figure 1 shows an SDSS composite image made with the *riz* filters in which the protostar and the faint nebulosity to the north can be seen.

A technical summary of the SDSS is given by York et al. (2000). The SDSS imaging camera is described by Gunn et al. (1998). The Early Data Release and the Data Release One are described by Stoughton et al. (2002) and Abazajian et al. (2003). The former includes an extensive discussion of the data outputs and software. Pier et al. (2003) describe the astrometric calibration of the survey and the network of primary photometric standard stars is described by Smith et al. (2002). The photometric system itself is defined by Fukugita et al. (1996), and the system which monitors the site photometricity by Hogg et al. (2001). Abazajian et al. (2003) discuss the differences between the native SDSS 2.5m *ugriz* system and the *u'g'r'i'z'* standard star system defined on the USNO 1.0 m (Smith et al. 2002).

The SDSS low Galactic latitude data which includes the Orion equatorial imaging used in this work are described by Finkbeiner et al. (2004).

The U.S. Naval Observatory Flagstaff Station 1.0 m and 1.55 m telescopes were used to obtain eruptive phase *BVRiz'* and *JHK* photometry of V1647 Ori. For *BVRiz'*, frames were taken and flatfielded using twilight sky flats. DAOPHOT PSF fitting as implemented in IRAF was used to obtain photometric measures of the target since there is a bright part of the nebula only a few arcsec distant. For each dataset, ensemble differential photometry was performed using a set of secondary standard stars calibrated on two photometric nights with the USNO 1.0 m telescope. The *z'* measures were relative to *z'* secondary standard stars calibrated by the SDSS PT telescope (Hogg et al. 2001). For *JHK*, we used 2MASS stars in the field, eliminating obvious variables, to calibrate the data. We used a standard *K* filter for 2004 February 11, but used a *K'* filter for 2004 April 12.

### 3. Results

The pre-eruptive and recent optical and near-infrared photometry of V1647 Ori are summarized in Tables 1, 2, and 3. The quiescent and eruptive phase spectral energy distributions are shown as  $\nu F_\nu$  in Figure 2.

We examine the evolution of reddening invariant colors from the quiescent to the eruptive states to constrain the underlying physical processes. These colors take the generic form  $C_{xyz} = (x - y) - (y - z) * E(x - y)/E(y - z)$  where *x*, *y*, and *z* are the observed magnitudes in each passband. A color change is computed as  $\Delta C_{xyz}$ , where color changes having  $\Delta C_{xyz}$  statistically distinct from 0 indicate changes in the spectral energy distribution (SED) not

consistent with pure dust clearing. The conversion from  $E(B - V)$  to extinction in each band follows Schlegel, Finkbeiner, & Davis (1998) and Finkbeiner et al. (2004), *in preparation*

The reddening invariant colors measured before and during the eruption are listed in Table 4 for both  $R_V = 3.1$  and  $R_V = 5.5$ , the latter appropriate for the larger dust grains found in star formation regions.  $R_V$ , defined as  $A_V/E(B - V)$ , is the ratio of the general to selective extinction.

Characteristic grain sizes are inferred to increase from  $0.17 \mu\text{m}$  to  $0.21 \mu\text{m}$  as  $R_V$  ranges from 3.1 to 5.5 assuming a mix of silicate and carbonaceous populations (Weingartner & Draine 2001). In the coldest portions of the molecular clouds additional grain species such as refractory and volatile organics, olivine, water ice, orthopyroxene, trolite, and metallic iron are expected to contribute to the opacity (Pollack et al. 1994). Vacca et al. (2004) detect absorption due to water ice at  $3.1 \mu\text{m}$  in the near-IR outburst spectrum.

Study of the selective extinction in background stars has revealed that  $R_V$  is not constant within the interiors of dark molecular clouds. Strafella et al. (2001) find that for the Bok globule CB 107  $R_V$  increases inwards reaching a value of 6.5 at the core. Given the complex nature of the V1647 Ori environment including outburst cavities, accretion disks, and remnant envelopes it is likely that  $R_V$  can vary on small spatial scales.

### 3.1. Determination of Extinction

In the foregoing analysis we choose to characterize the intervening dust in terms of the SDSS  $z$  band extinction and  $R_V$ . Since the shape of the extinction curve is dependent upon the grain size distribution for  $\lambda < 0.9 \mu\text{m}$  (Cardelli, Clayton & Mathis 1989) the traditional  $A_V$  and  $E(B - V)$  quantities are sensitive to both the dust column density and  $R_V$ . By adopting reference passbands longward of  $0.9 \mu\text{m}$  we remove the dependency on the form of the dust law although  $R_V$  must still be considered in the optical and UV. Alternate passbands that are free of  $R_V$  effects include the near-IR  $J$  and Johnson-Cousins  $I$ , the latter used by Weingartner & Draine (2001) who adopted  $A_I/N(\text{HI}) = 2.5 \times 10^{-22} \text{ cm}^2$  for a standard gas-to-dust ratio.

Following Abraham et al. (2004) and Reipurth & Aspin (2004) we assume that the quiescent phase near-IR colors are that of an embedded low-mass Classical T Tauri and obtain  $E(J - H) = 1.43^m$  by dereddening onto the Classical T Tauri locus of Meyer, Calvet, & Hillenbrand (1997). This value of  $E(J - H)$  corresponds to  $A_J = 3.39^m$  ( $A_z = 6.40^m$ ) given  $\lambda_{\text{eff}}(J) = 1.25 \mu\text{m}$  and  $\lambda_{\text{eff}}(H) = 1.65 \mu\text{m}$  and application of the Cardelli, Clayton & Mathis (1989) methodology.

### 3.2. Changes in the Spectral Energy Distribution

In order to analyze the general differences between the quiescent and eruptive appearance we combine sets of observations to form representative values. The quiescent state is taken as the October 7 (2MASS  $J, H, K$ ) and the 1998 November 17 (SDSS  $r, i, z$ ) observations. The optical photometry for the eruptive state is obtained from the 2004 February 14 Gemini  $r$  and  $i$  data (Reipurth & Aspin 2004), and the 2004 February 26 USNO  $z$  band observations. The  $J, H$ , and  $K$  data for the eruptive state are from the 2004 February 11 USNO observations.

Table 5 presents the reddening invariant colors in the quiescent and eruptive states for  $R_V = 3.1$  and  $R_V = 5.5$ . As evidenced by the greater than  $5\sigma$  change in all colors except for  $C_{riz}$ , which has a marginal  $r$  band detection in the quiescent state, it is clear that the increase in emission is not consistent with a dust clearing event and thus we conclude that an intrinsic change occurred to the SED of V1647 Ori.

In Figure 3 we compare the observed magnitude variations against  $\Delta A_z = -2^m$  and  $-4^m$  dust clearing events and, as concluded above based on reddening invariant colors, find they are not explainable in terms of a simple diminishing of the line of sight extinction.

### 3.3. The Quiescent Phase

From observations of Class II protostars (Classical T Tauris) we would expect that the veiling continuum due to magnetospheric accretion will be present in the SDSS  $u$  and  $g$  bands but weakening into the redder  $r$ ,  $i$  and  $z$  bands (Calvet & Gullbring 1998). In a similar fashion, the thermal emission from the inner portion of the circumstellar disk should be bright in the  $H$  and  $K$  bands but diminishing into the bluer  $J$  band (Meyer, Calvet, & Hillenbrand 1997). For all but the mostly heavily veiled stars the  $i$  and  $z$  bands will only be affected by extinction. None of the reddening invariant colors can be used to give the intrinsic spectral type.

Young (1 Myr) T Tauri stars exhibit spectral types between M0 and M4 for masses of 0.1 to 1.0  $M_\odot$  (Baraffe et al. 1998). The use of the Meyer, Calvet, & Hillenbrand (1997) near-IR Classical T Tauri locus by Abraham et al. (2004) and Reipurth & Aspin (2004) implicitly assumes a similar spectral type as this locus is based on observations of K7/M0 stars in the Taurus star formation region. The  $i - z$  colors for these early to mid M spectral types range from 0.38 to 0.80 with considerable scatter on the order of several tenths of magnitudes (West et al. 2004). Given the observed  $i - z$  ( $2.01 \pm 0.06$ ), dereddening to these intrinsic colors requires  $A_z = 3.1^m$  to  $4.2^m$  for  $R_V = 3.1$  and  $4.3^m$  to  $5.7^m$  for  $R_V = 5.5$ .

Dereddening using the estimated  $A_z \sim 6.4$  and  $R_V = 3.1$  results in an intrinsic  $i - z$  of -0.47, which is too blue for the stellar locus. Assumption of  $R_V = 5.5$  yields an  $i - z$  of 0.20, corresponding to a late K spectral type (Finlator et al. 2000). If V1647 Ori is indeed a low mass protostar with a late K or M spectral type then either  $R_V$  is high or significant  $i$  band veiling is present in the quiescent state.

In Figure 4 we compare the observed quiescent phase SED against an M0 photosphere seen under an extinction of  $A_z=6.4$  magnitudes. Excess emission is seen in the  $J$ ,  $H$ , and  $K$  bands that could indicate the presence of a circumstellar disk.

### 3.4. The Eruptive Phase

The optical spectra acquired during the outburst by Walter et al. (2004) lack the TiO molecular absorption bands characteristic of late K and M stars. Walter et al. (2004) attribute this to either an early photospheric spectral type or overwhelming veiling. We adopt the latter interpretation given the apparent change to the intrinsic SED and the large brightness increase in the optical (Figure 3).

If the new component to the SED is due to an EXor outburst then we expect to see emission from the high temperature (6000 - 8000 K) inner disk (Bell et al. 1995). In Figure 5 we show the observed flux ( $\nu F_\nu$ ) increase in comparison with a 7000 K blackbody reddened by  $A_z = 3.2^m$  and  $6.4^m$  for  $R_V = 3.1$  and 5.5. In common with Walter et al. (2004) we see that a single EXor-like high temperature component can not reproduce the observed excess in both the optical and the near-IR.

For the partial dust clearing events suggested by Reipurth & Aspin (2004) and Walter et al. (2004) we find that due to the increase in optical depth towards the blue the additional flux due to a new source must fall more rapidly at the shorter wavelengths. The observed change in  $J - H$  is  $-0.61^m$ , which if entirely due to dust clearing requires  $\Delta A_z = -3.2^m$ . The intrinsic flux increase required in this case is shown in Figure 5 and would require either a lower temperature for the new source or a significantly higher extinction than anticipated.

Spectral indices are commonly defined by the ratio of the flux of the feature ( $F_s$ ) and that of the nearby pseudo-continuum ( $F_c$ ), so the intrinsic measure of the feature strength is  $I_0 = F_s/F_c$  (Gizis 1997). If a veiling continuum is present, defined by  $F_v = rF_c$ , then the measured spectral index,  $I$ , is



$$\begin{aligned}
 I &= \frac{F_s + rF_c}{F_c + rF_c} \\
 &= \frac{I_0}{1 + r} + \frac{r}{1 + r}.
 \end{aligned} \tag{1}$$

Figure 6 shows the observed depression of the line relative to the continuum level ( $1 - I$ ) on a logarithmic scale as a function of the veiling,  $r$ , for unveiled indices of  $I_0 = 0.0, 0.1$ , to  $0.9$ . From Figure 3 we see that the flux in the  $i$  band has increased by  $\Delta m = -5$  or a factor of  $\sim 100$  which means the TiO features will be visible as less than a 1% fluctuation in the observed continuum.

#### 4. Conclusions

The observed photometric variations are not consistent with a simple dust clearing event as evidenced by changes in reddening invariant indices. We infer that the process of eruption involves changes to both the optical and near-IR SED.

Application of an inferred pre-outburst extinction of  $A_z = 6.4^m$  suggests a late K spectral type if the  $r - i$  and  $i - z$  colors are minimally affected by the veiling continuum arising from magnetospheric accretion shocks and that  $R_V$  has a value expected for a star formation region. An early to mid M spectral type is possible if the  $i$  band includes an excess emission of  $0.2^m$  to  $0.6^m$ , corresponding to a veiling between 0.2 and 0.7.

We interpret the quiescent phase of V1647 Ori as an embedded low mass Classical T Tauri. Comparison with a reddened M0 photosphere shows a near-IR excess that is presumably due to thermal emission from a normal circumstellar disk.

The outburst SED is dominated by the new component. We see that a single blackbody having the  $\sim 7000$  K temperature expected for an EXor inner disk can not simultaneously reproduce both the optical and near-IR portions of the SED. It is possible, as suggested by Reipurth & Aspin (2004), that a partial dust clearing event occurred in combination with an intrinsic brightening. We note that a reduction of the line of sight extinction would preferentially lessen the required flux increase at shorter wavelengths. This steepening of the curve shown in Figure 5 would increase the difficulty of fitting the high temperature (B spectral type) component observed by Briceño et al. (2004).

Further study of V1647 Ori planned using the facilities at USNO, Apache Point Observatory, and the Spitzer Space Telescope may clarify the nature and evolutionary state of this young star.

Funding for the creation and distribution of the SDSS Archive has been provided by the Alfred P. Sloan Foundation, the Participating Institutions, the National Aeronautics and Space Administration, the National Science Foundation, the U.S. Department of Energy, the Japanese Monbukagakusho, and the Max Planck Society. The SDSS Web site is <http://www.sdss.org/>.

The SDSS is managed by the Astrophysical Research Consortium (ARC) for the Participating Institutions. The Participating Institutions are The University of Chicago, Fermilab, the Institute for Advanced Study, the Japan Participation Group, The Johns Hopkins University, Los Alamos National Laboratory, the Max-Planck-Institute for Astronomy (MPIA), the Max-Planck-Institute for Astrophysics (MPA), New Mexico State University, University of Pittsburgh, Princeton University, the United States Naval Observatory, and the University of Washington.

This publication makes use of data products from the Two Micron All Sky Survey, which is a joint project of the University of Massachusetts and the Infrared Processing and Analysis Center/California Institute of Technology, funded by the National Aeronautics and Space Administration and the National Science Foundation.

Finally we thank the referee, Colin Aspin, for his helpful comments.

Facilities: SDSS, USNO, Gemini-N, 2MASS.

## REFERENCES

- Abazajian, K., et al. 2003, *AJ*, 126, 2081
- Abraham, P. et al. 2004, *A&A*, 419L, 39
- Andrews, S.M., Rothberg, B., & Simon, T. 2004, *ApJ*, 610, 45
- Anthony-Twarog, B.J. 1982, *AJ*, 87, 1213
- Baraffe, I. et al. 1998, *A&A*, 337, 403
- Bell, K.R. et al. 1995, *ApJ*, 444, 376
- Briceño, C. et al. 2004, *ApJ*, 606, 123
- Calvet, N. & Gullbring, E. 1998, *ApJ*, 509, 802
- Cardelli, J.A., Clayton, G.C., & Mathis, J.S. 1989, *ApJ*, 345, 245
- Clark, F. O. 1991, *ApJS*, 75, 611
- Eislöffel, J. & Mundt, R. 1997, *AJ*, 114, 280
- Finkbeiner, D. et al. 2004, *AJ*, submitted
- Finlator, K. et al. 2000, *AJ*, 120, 2615
- Fukugita, M., Ichikawa, T., Gunn, J.E., Doi, M., Shimasaku, K., & Schneider, D.P. 1996, *AJ*, 111, 1748
- Gizis, J.E. 1997, *AJ*, 113, 806
- Gunn, J.E. et al 1998, *AJ*, 116, 3040
- Herbig, G.H. 1977, *ApJ*, 217, 693
- Herbig, G.H. et al. 2001, *PASP*, 113, 1547
- Hodapp, K-W. et al. *ApJ*, 468, 861
- Hogg, D.W., Finkbeiner, D.P., Schlegel, D.J., & Gunn, J.E. 2001, *AJ*, 122, 2129
- Lis, D.C., Menten, K.M., & Zylka, R. 1999, *ApJ*, 527, 856
- McNeil, J.W. 2004, *IAUC* 8284, 9 February 2004.

- Meyer, M.R., Calvet, N, & Hillenbrand, L.A. 1997, AJ, 114, 288 ApJ, 266, 713
- Pier, J.R., Munn, J.A., Hindsley, R.B., Hennessy, G.S., Kent, S.M., Lupton, R.H., & Ivezić, Ž. 2003, AJ, 125, 1559
- Pollack, J.B. et al. 199), ApJ, 421, 615
- Reipurth, B. & Aspin, C. 2004, ApJ, 606, 119
- Schlegel, D., Finkbeiner, D. & Davis, M. 1998, ApJ, 500, 525
- Smith, J.A., et al 2002, AJ, 123, 2121
- Stoughton, C., et al 2002, AJ, 123, 485
- Strafella, F. et al. 2001, ApJ, 558, 717
- Vacca, W.D. et al. 2004, ApJ, 609, 29
- Walter, F.M et al. 2004, astro-ph/0406618
- Weingartner, J.C. & Draine, B.T. 2001, ApJ, 548, 296
- West, A. et al 2004, AJ, 128, 426
- York, D. et al. 2000, AJ, 120, 1579

Table 1. *riz* Photometry of V1647 Ori

Date	<i>r</i>	<i>i</i>	<i>z</i>	Telescope
1998 Nov 17	$23.04 \pm 0.22$	$20.81 \pm 0.05$	$18.80 \pm 0.04$	SDSS
1998 Nov 28	$24.00 \pm 0.80$	$21.03 \pm 0.09$	$19.19 \pm 0.08$	SDSS
2002 Feb 07	$22.69 \pm 0.29$	$20.77 \pm 0.08$	$18.77 \pm 0.06$	SDSS
2002 Feb 09	$23.88 \pm 0.73$	$21.33 \pm 0.11$	$19.33 \pm 0.07$	SDSS
2004 Feb 14	17.4	15.6	...	Gemini <sup>a</sup>
2004 Feb 26	...	...	$14.60 \pm 0.06$	USNO 1.55m
2004 Apr 16	...	...	$14.79 \pm 0.06$	USNO 1.55m
2004 Apr 27	...	...	$14.72 \pm 0.09$	USNO 1.55m

<sup>a</sup>From Reipurth & Aspin (2004).

Table 2. Johnson-Cousins Photometry of V1647 Ori

Date	$B$	$V$	$R_c$	$I_c$	Telescope
2004 Feb 11	...	$18.52 \pm 0.07$	$16.91 \pm 0.08$	$14.92 \pm 0.05$	USNO 1.0m
2004 Feb 16	$20.39 \pm 0.12$	$18.59 \pm 0.06$	$16.87 \pm 0.07$	$14.90 \pm 0.04$	USNO 1.0m
2004 Feb 25	...	$18.68 \pm 0.04$	...	...	USNO 1.55m
2004 Feb 26	$20.84 \pm 0.08$	$18.99 \pm 0.04$	...	$15.15 \pm 0.02$	USNO 1.55m
2004 Apr 13	$20.74 \pm 0.33$	$19.12 \pm 0.08$	$17.24 \pm 0.09$	$15.28 \pm 0.05$	USNO 1.0m
2004 Apr 16	$21.13 \pm 0.07$	$19.26 \pm 0.03$	...	$15.37 \pm 0.01$	USNO 1.55m

Table 3. Near-IR Photometry of V1647 Ori

Date	$J$	$H$	$K$	Telescope
1998 Oct 07	$14.74 \pm 0.03$	$12.16 \pm 0.03$	$10.27 \pm 0.02$	2MASS
2004 Feb 03	$11.1 \pm 0.1$	$9.0 \pm 0.1$	$7.4 \pm 0.1$	Gemini <sup>a</sup>
2004 Feb 11	$10.79 \pm 0.01$	$8.83 \pm 0.01$	$7.72 \pm 0.01^b$	USNO 1.55m
2004 Apr 12	$10.94 \pm 0.02$	$9.06 \pm 0.02$	$7.59 \pm 0.02^b$	USNO 1.55m

<sup>a</sup>From Reipurth & Aspin (2004).

<sup>b</sup>The USNO 1.55m observations used standard  $K$  on 2004 February 11 and  $K'$  on 2004 April 12, both placed on the 2MASS zeropoint system, but probably with transformation differences.

Table 4. Reddening Invariant Colors

Color	$R_V = 3.1$	$R_V = 5.5$
$C_{riz}$	$(r - i) - 0.987 * (i - z)$	$(r - i) - 1.002 * (i - z)$
$C_{izJ}$	$(i - z) - 0.824 * (z - J)$	$(i - z) - 0.605 * (z - J)$
$C_{zJH}$	$(z - J) - 2.443 * (J - H)$	$(z - J) - 2.443 * (J - H)$
$C_{JHK}$	$(J - H) - 1.563 * (H - K)$	$(J - H) - 1.563 * (H - K)$



Table 5. Reddening Invariant Color Changes

Color	$R_V = 3.1$			$R_V = 5.5$		
	Quiescent <sup>a</sup>	Eruptive <sup>b</sup>	$N\sigma^c$	Quiescent <sup>a</sup>	Eruptive <sup>b</sup>	$N\sigma^c$
$C_{riz}$	$0.25 \pm 0.23$	$0.81 \pm 0.10$	2.2	$0.22 \pm 0.23$	$0.80 \pm 0.11$	2.3
$C_{izJ}$	$-1.34 \pm 0.08$	$-2.14 \pm 0.09$	-6.7	$-0.45 \pm 0.07$	$-1.31 \pm 0.09$	-7.7
$C_{zJH}$	$-2.24 \pm 0.12$	$-0.98 \pm 0.07$	9.4	$-2.24 \pm 0.12$	$-0.98 \pm 0.07$	9.4
$C_{JHK}$	$-0.37 \pm 0.07$	$0.23 \pm 0.03$	8.0	$-0.37 \pm 0.07$	$0.23 \pm 0.03$	8.0

<sup>a</sup>The quiescent state is defined by the 1998 October 7 2MASS and 1998 November 17 SDSS data.

<sup>b</sup>The eruptive phase data are from the 2004 February 14 Gemini  $r$  and  $i$ , the 2004 February 26 USNO  $z$ , and the 2004 February 11 USNO  $J$ ,  $H$ , and  $K$  measurements.

<sup>c</sup> $N\sigma$  is the ratio of color change to the quadrature sum of measurement errors.

Fig. 1.— **SDSS pre-eruption *riz* band mosaic image of V1647 Ori.** The location of V1647 Ori is marked on this 2x2 binned mosaic which maps the SDSS *r*, *i*, and *z* bands onto blue, green, and red. Herbig-Haro objects, such as the large HH 24 complex (*bottom center*), are seen in blue due to the H $\alpha$  emission appearing in the *r* band. The image is roughly 10 arcminutes on a side and is displayed using a negated grayscale. North is up and east is to the left. The faint emission immediately north of V1647 Ori significantly brightens during the eruptive phase where it is seen as McNeil’s Nebula. The diffuse *r* band emission due to HH 23, which may be driven by V1647 Ori, is highlighted by the box in the upper center. *A color rendition of this image is available in the electronic version of the journal.*

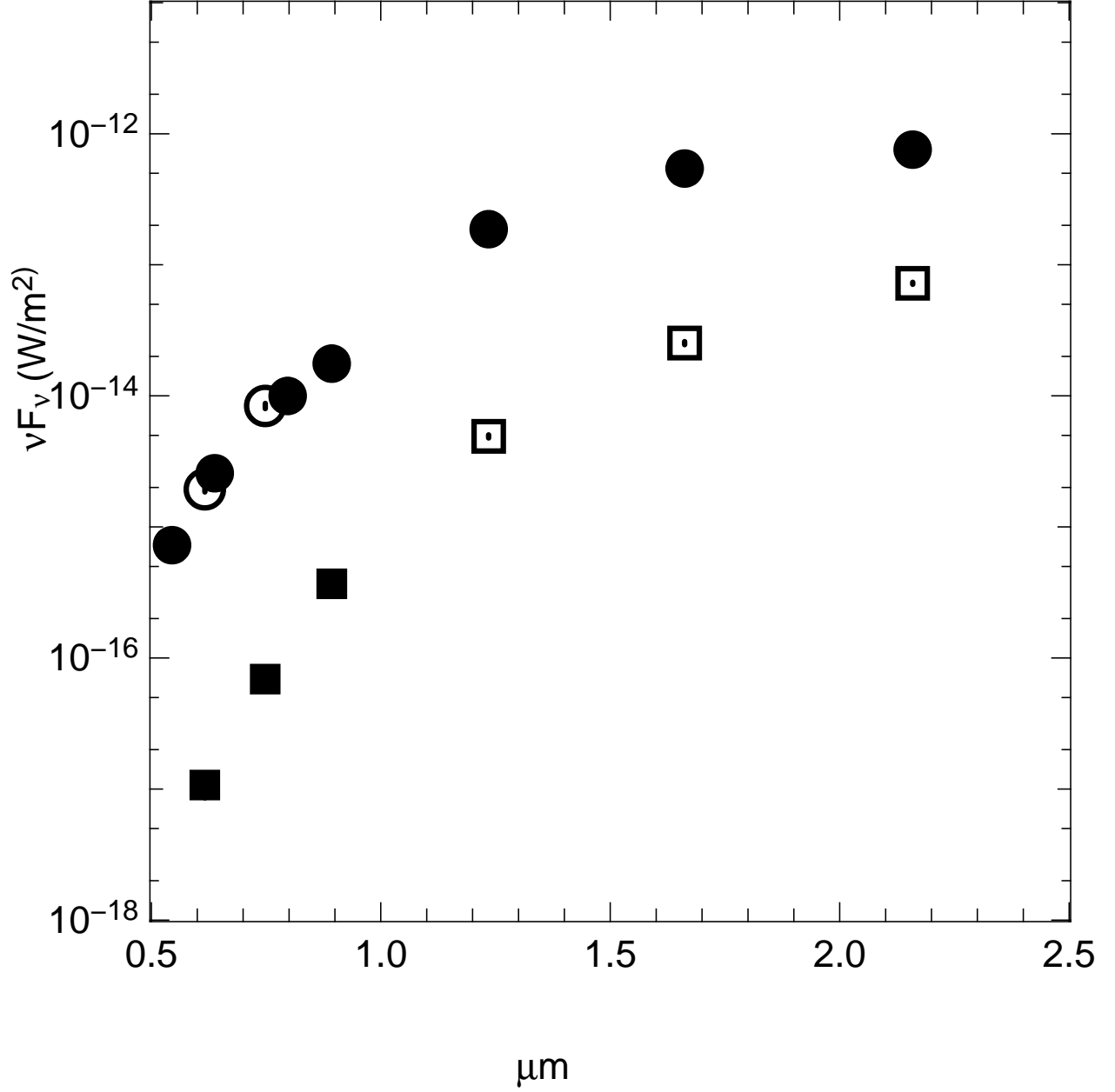


Fig. 2.— **Quiescent and Eruptive Spectral Energy Distributions.** The optical and near-IR SEDs are shown for the quiescent state (*squares*) and during eruption (*circles*). Data acquired by the SDSS and at the USNO are indicated by filled symbols. The open squares are the 2MASS *JHK* observations and the open circles are the *r* and *i* band eruptive phase measurements of Reipurth & Aspin (2004).

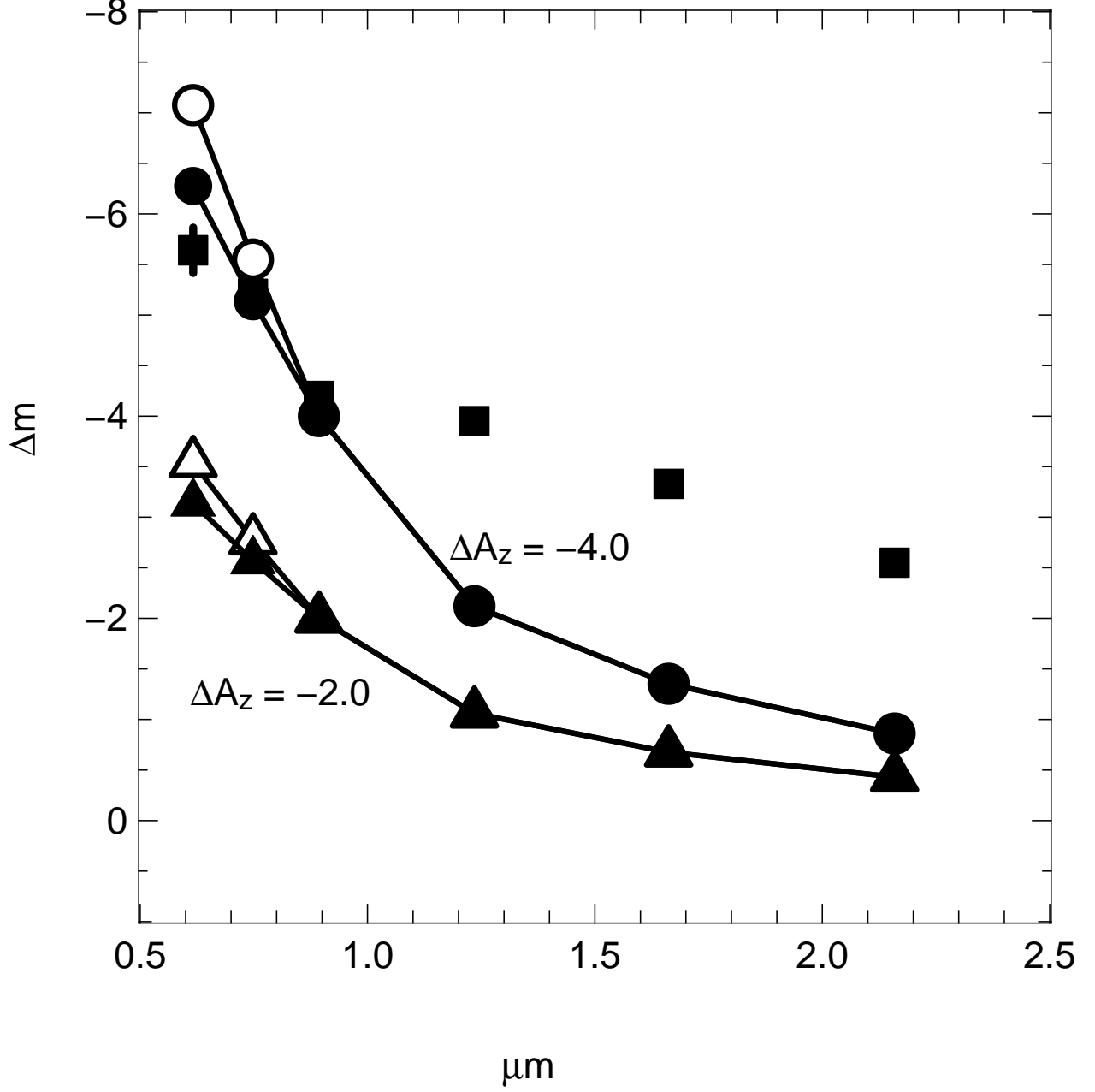


Fig. 3.— **Changes in Spectral Energy Distributions.** The observed magnitude differences (*squares*) are compared against pure dust clearing events for  $\Delta A_z = -2^m$  (*circles*) and  $\Delta A_z = -4^m$  (*triangles*) and for  $R_V = 3.1$  (*solid*) or  $R_V = 5.5$  (*open*) dust laws.

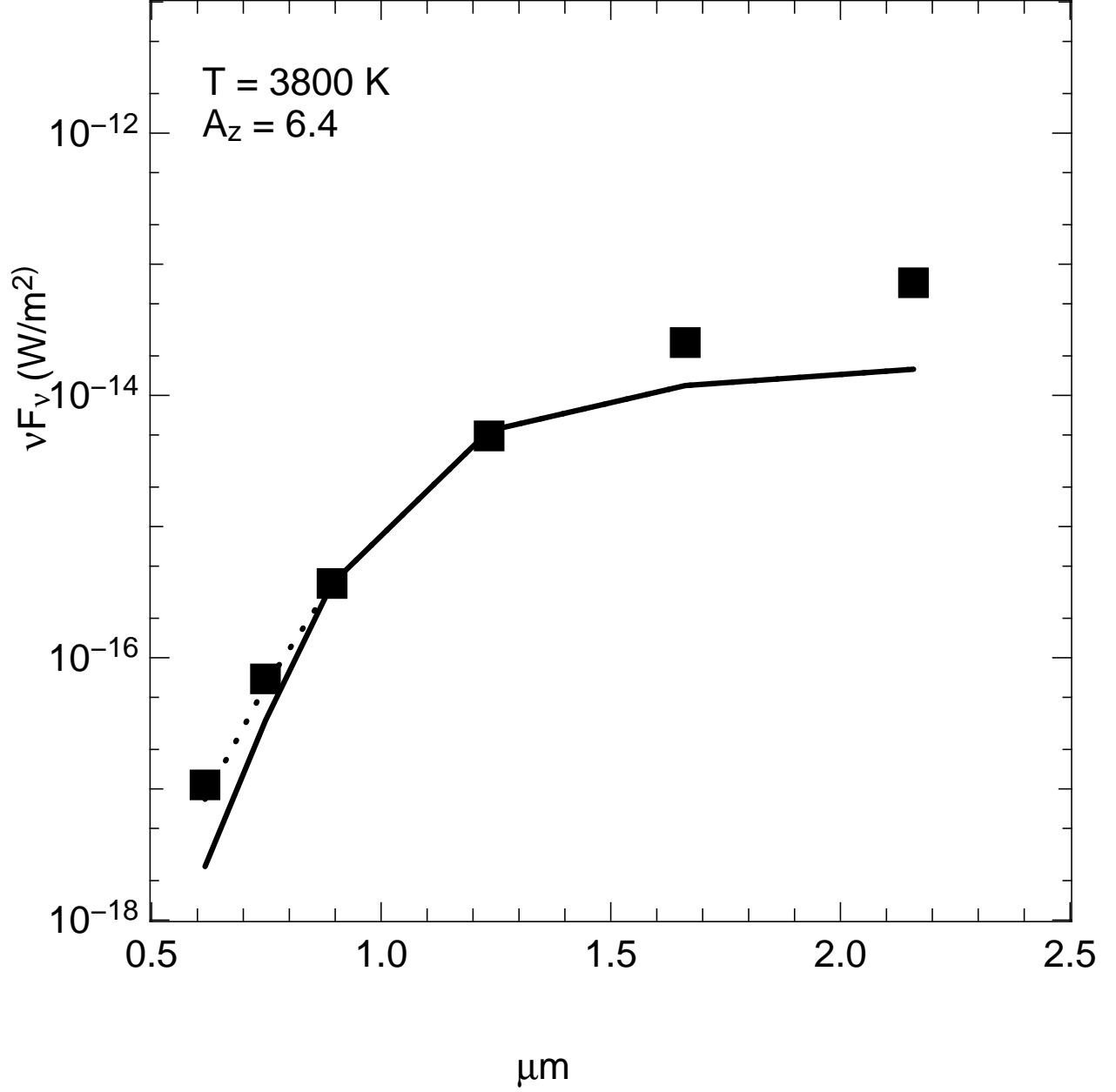


Fig. 4.— **Modeling the Quiescent Spectral Energy Distribution.** Observed pre-eruption SED compared with an M0 photosphere (3800 K) seen under a line of sight reddening of  $A_z = 6.4^m$  for  $R_V = 3.1$  (*solid line*) and  $R_V = 5.5$  (*dotted line*). Excess emission is evident longward of  $1.2 \mu\text{m}$  (*J*).

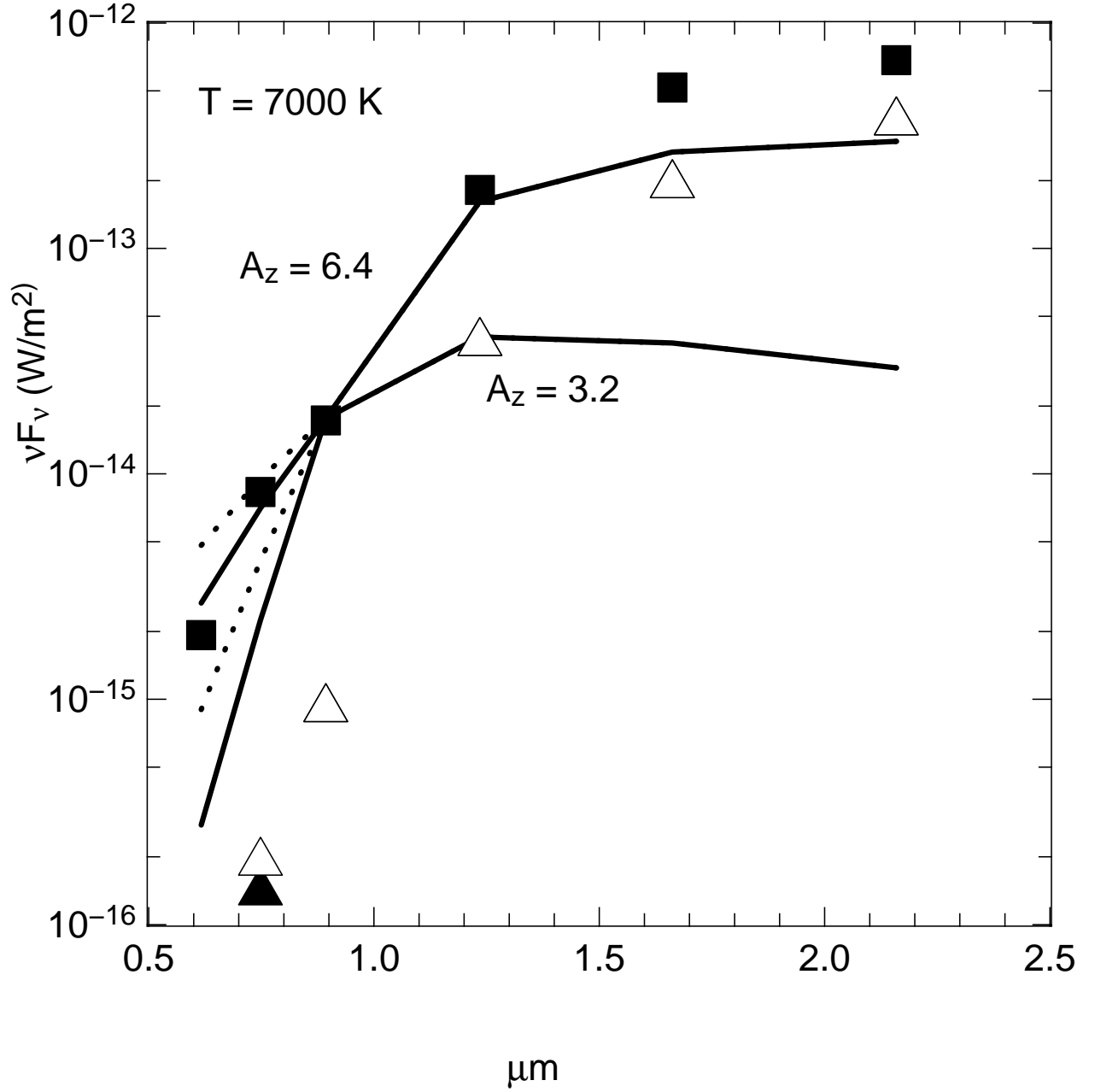


Fig. 5.— **Modeling the Eruptive Component.** This figure compares the observed flux increase (*filled squares*) against a 7000 K blackbody viewed under ( $R_V=3.1$  (*solid*),  $5.5$  (*dotted*)) extinctions of  $A_z = 3.2^m$  and  $6.4^m$ , scaled to match the observed change in the  $z$  band flux. The triangles show the required intrinsic flux increase in the case of a  $\Delta A_z = -3.2^m$  partial dust clearing for  $R_V = 3.1$  (*filled*) and  $5.5$  (*open*).

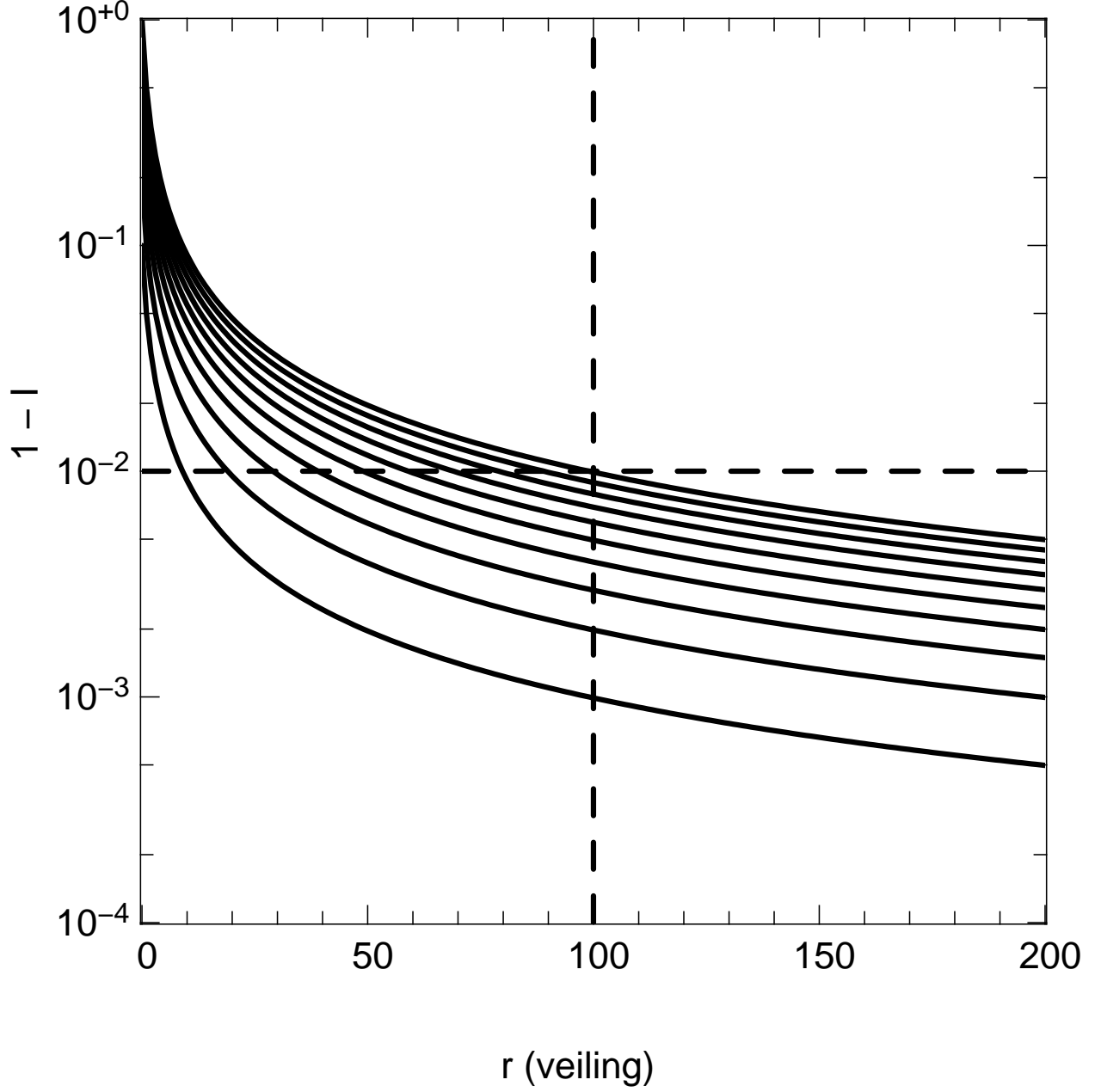


Fig. 6.— **Effect of Veiling on Spectral Features.** This figure plots the observed depression of an absorption line relative to the continuum level ( $1 - I$ ) on a logarithmic scale as a function of the veiling,  $r$ , for unveiled indices of  $I_0 = 0.0, 0.1$ , to  $0.9$ . The dashed lines indicate the eruptive phase  $i$  band veiling of 100 and a relative depression level of 1%.

This figure "f1COLOR.jpg" is available in "jpg" format from:

<http://arxiv.org/ps/astro-ph/0408308>